Post print of TASSONE, Alessandro, et al. Recent progress in the WCLL breeding blanket design for the DEMO fusion reactor. IEEE Transactions on Plasma Science, 2018, 46.5: 1446-1457. Doi: https://doi.org/10.1109/TPS.2017.2786046

Recent progress in the WCLL breeding blanket design for the DEMO fusion reactor

Alessandro Tassone, Alessandro Del Nevo, Pietro Arena, Gaetano Bongiovì, Gianfranco Caruso, Pietro Alessandro Di Maio, Giuseppe Di Gironimo, Marica Eboli, Nicola Forgione, Ruggero Forte, Fabio Giannetti, Giovanni Mariano, Emanuela Martelli, Fabio Moro, Rocco Mozzillo, Andrea Tarallo, Rosaria Villari

***Abstract*—The water-cooled lithium lead breeding blanket is one of the candidate systems considered for the implementation in the European Demonstration Power Plant (DEMO) nuclear fusion reactor. This concept employs lithium-lead liquid metal as tritium breeder and neutron multiplier, water pressurized at 15.5 MPa as the coolant, and EUROFER as the structural material. The current design is based on the Single Module Segment approach and follows the requirements of the DEMO-2015 baseline design. The module is constituted by a basic toroidal-radial cell that is recursively repeated along the poloidal direction where the liquid metal flows along a radial-poloidal path. The heat generated by the fusion reactions is extracted by means of separate cooling systems for the breeding zone and the first wall. A back supporting structure is dedicated to withstand loads of the module during normal and off-normal operations. Water and lithium-lead manifolds are integrated with primary heat transport and tritium extraction systems. The status of the conceptual design is presented, critically discussing its rationale and main features as supported by neutronic, thermal-hydraulic, magneto-hydrodynamic and thermo-mechanic analyses. Recent results are outlined, pointing out open issues and development needs.**

***Index Terms*—Breeding blanket, DEMO, Fusion reactor design, Liquid metal technology**

I. Introduction

One of the most important components of a magnetic confinement fusion power plant, the breeding blanket (BB), must provide tritium self-sufficiency, heat extraction and transportation to the primary heat transfer system (PHTS) and neutron shielding while withstanding extreme environmental conditions. The blanket system features will impact the Demonstration Power Plant (DEMO) design, availability, safety and economics [1].

One of the four BB concepts considered for the EU DEMO, the water-cooled lithium-lead (WCLL) blanket, relies on EUROFER as structural material, liquid eutectic lithium-lead (PbLi) enriched at 90% in Li^6 as tritium breeder and neutron multiplier, water as coolant for both the first wall (FW) and the breeding zone (BZ) [2]. Coolant thermodynamic conditions are based on the well-known pressurized water fission reactor cycle. Design activities are conducted to develop a feasible and integrated conceptual design of the WCLL BB in the framework of the Horizon 2020 EUROfusion Project [3].

Starting from the experience accumulated through the studies carried over in the past years [4]–[7], the WCLL BB Design 2016 follows a Single Module Segment baseline approach where the liquid metal flows in an elementary cell that is repeated in the module along the poloidal direction. This configuration has several advantages compared with the Multi-Module Segment one, among which easier PbLi drainage, evacuation of helium generated by the tritium breeding reaction, simpler manifold integration and increased Tritium Breeding Ratio (TBR) [7].

In this paper, the design features and performances evaluated by means of neutronic, thermal-hydraulic, thermo-mechanic and magnetohydrodynamic (MHD) analyses are reported and critically discussed with the outline of open issues and areas of research that still require careful consideration.

II. WCLL Design description

The 2016 configuration of DEMO WCLL BB is designed using a single module approach. In other words, each segment of BB is conceived as one single box, deeply differing from the previous configuration segmented in the poloidal direction in several modules connected to a common back supporting structure joined to the Vacuum Vessel [8].

The design of WCLL BB has been developed through a parametric approach [9], to allow easy exchange of data between different modeling and analysis environments, as

This work has been carried out within the framework of the EUROfusion Consortium and has received funding from the Euratom research and training programme 2014-2018 under grant agreement No633053. The views and opinions expressed herein do not necessarily reflect those of the European Commission.

A. Tassone, G. Caruso, F. Giannetti, E. Martelli and G. Mariano are with DIAEE, Sapienza University of Rome, Corso Vittorio Emanuele II, 244, 00186 Rome, Italy.

A. Del Nevo is with ENEA FSN-ING-PAN, ENEA CR Brasimone, Località Brasimone, 40032 Camugnano, BO, Italy (e-mail: alessandro.delnevo@enea.it)

P. Arena, G. Bongiovì, P. A. Di Maio and R. Forte are with University of Palermo, Viale Delle Scienze, Edificio 6, 90128 Palermo, Italy.

G. Di Gironimo, R. Mozzillo, and A. Tarallo are with CREATE, University of Naples Federico II, DII, P.le Tecchio 80, 80125 Naples, Italy.

M. Eboli and N. Forgione are with DICI, University of Pisa, Largo Lucio Lazzarino 2, 56122 Pisa, Italy.

F. Moro and R. Villari are with ENEA FSN-FUSTEC-TEN, ENEA CR Frascati, via E. Fermi 45, 00044 Frascati, Italy.

already successfully experienced for other DEMO key components [10].

In the 2016 configuration, five segments compose each DEMO sector (20°), two placed on the inboard side and the other three on the outboard side.

The geometry of the modules is simplified to address, as much as possible, manufacturing issues.

The single BB module is composed of the following components:

- First Wall (FW) and Side Walls (SW)
- Top and Bottom walls
- Internal Stiffening and Baffle Plates
- Back Plate
- Breeding Zone (BZ) cooling pipes
- Lithium Lead (PbLi) manifold
- BZ Inlet and Outlet cooling manifolds
- FW Inlet and Outlet cooling manifolds

Each DEMO sector is fed by the piping system through the upper and lower port (Fig. 1).

The First Walls (FWs) of the modules (inboard and outboard) are single curved in poloidal direction. Their thickness is 25 mm and they are cooled by square channels arranged so to assure the symmetry of the module cells. Moreover, the cooling water flows in the FWs channels in countercurrent along a radial-toroidal path.

The FWs are covered by a tungsten layer of 2 mm in thickness on the plasma facing area.

To guarantee the structural integrity of each segment against the over pressurization, the WCLL BB modules (inboard and outboard) are equipped with internal stiffening plates placed along poloidal-radial (PR) and toroidal-radial (TR) planes. In detail each module (inboard and outboard) has five PR stiffening plates 16-mm thick and about 100 TR ribs 12-mm thick (Fig. 2).

To facilitate PbLi circulation, about 100 2 mm-thick baffle plates have been placed, with a toroidal-radial layout, inside each module for both the inboard and the outboard side.

The distance between TR stiffening plates and baffle plates is 135 mm and is calculated on a curvilinear coordinate. The TR ribs and baffle plates are planar and locally normal to the plasma-facing BB profile (Fig. 3).

The position of FWs channels is symmetrical with respect to the plane of TR and baffle plates.

This internal layout generates for each BB module about 100 TR single cells. The Breeding Zone cooling tubes (Fig. 4) are placed in each cell. They are double walled and have external/internal diameters of 13.5/8 mm.

The BZs for the inboard and outboard modules are respectively 450 mm and 800 mm thick in the radial direction (Fig. 5).

The PbLi manifolds are placed inside the modules structures and their walls are 30 mm thick (Fig. 5 and Fig. 6).

The back plates of the modules are properly cut in the back area to save space for the BZ and FW cooling water manifolds (Fig. 6 and Fig. 7**)**.

The back supporting structures (BSS) of the modules (inboard and outboard) are T-shaped and joined to the sidewalls and the back plates of the modules. In particular, the BSS is connected to the back-plate of each module through a proper rib of 250 mm in thickness.

Water coolant is fed to the five modules of each DEMO sector by a dedicated piping system. The pipes are routed through the upper of DEMO Vacuum Vessel. Two solutions for the feeding pipes layout are currently under investigation:

- feeding pipes with toroidal collectors on the top area of BB segments
- feeding pipes without toroidal collector on the top area of BB segments

In the first configuration, the feeding pipes system is equipped with toroidal collectors placed between the Vacuum Vessel and BB sector. These collectors are fed by vertical pipes dimensioned to guarantee the envisioned flow rate avoiding an unduly high pumping power (Fig. 8). Each collector feeds three modules at the outboard and two modules at the inboard.

The effect of this design choice consists in a reduction of the number of feeding pipes since just one pipe for each input and output feeding line is needed. The upper port contains the inlet and outlet pipes of the cooling water (FW and BZ) and the inlet pipe of PbLi while the outlet pipes of PbLi have been placed in the lower port. Currently, this configuration is under study to face issues related to BB remote maintenance.

In the configuration with feeding pipes without toroidal collector on the top area of BB segments, each sector is fed by a single tube for the inlet and one for the outlet lines. Indeed the number of the feeding pipes inside the upper port increases by a factor 5 with respect to the previous one (Fig. 1).

Moreover, single modules have been equipped with an additional manifold to distribute the PbLi uniformly inside the BZ (Fig. 9 and Fig. 10).

The additional manifold is placed between the BSS and the BZ manifolds just on the top area of each segment (Fig. 9).

As in the previous configuration, the lower port contains only the PbLi outlet pipes as shown in Fig. 1.

III. Neutronic Activities

The neutronic analyses carried out in support of the WCLL breeding blanket design are aimed at verifying the nuclear performances of the present layout of the blanket concept, providing feedback for its future development.

The main objective of the neutronic studies is the assessment of the WCLL DEMO tritium self-sufficiency and evaluation of the breeding blanket/manifold system shielding capabilities. Moreover, the radial profiles of the nuclear loads (neutron flux, nuclear heating, neutron damage and helium production) have been assessed at the equatorial level, providing an indication about their behavior on the FW, BB, supporting structures and manifolds that have been used ad input data for the thermo-hydraulic and thermo-mechanical analyses.

Neutronics studies carried-out in 2015 were based on the multi-module DEMO configuration, integrating a WCLL breeding blanket represented by homogenized compounds. The present studies have been performed using an upgraded MCNP WCLL DEMO model, introducing a detailed description of the

breeding blanket in the inboard and outboard equatorial modules, thus allowing a more realistic and reliable particle transport in the mid-plane area of the tokamak. Three dimensional coupled neutron and gamma transport simulations have been performed according to specific guidelines [11], [12] by means of the MCNP5v1.6 Monte Carlo code [13] and JEFF 3.2 nuclear data libraries [14].

The outcome of the performed studies [7] highlighted the following issues:

- the design target for self-sufficiency is fully satisfied, being the total TBR about 1.184. Most of the tritium (99.7%) is produced in the breeder zone, while the remaining 0.03% is generated in the back-plate. With respect to previous analyses, the contribution of the manifolds to the tritium production is negligible, because, according to the latest development of the WCLL breeding blanket, the LiPb inlet/outlet piping system feed the blanket from the lower port, through the back wall of the modules. The poloidal distribution of the TBR showed that the peak value is obtained in the equatorial modules, with the TBR varying from 3% to 4% with respect to the results obtained for the equatorial segments using homogenized materials. This effect is attributable to the detailed heterogeneous and more realistic description of the blanket integrated with those sectors;
- the combined blanket/manifold/VV system is sufficient to protect the toroidal field coils (TFC) from the radiation streaming: the fast neutron flux evaluated on the TFC winding pack is 2.9×10^{8} n/cm^2/s (design target: 10^9 n/cm^2/s), and the nuclear heating is 1.4x10-5 W/cm^3 (design target: 50 W/m^3).
- the damage on the VV stainless steel is ~6.2x10-3 dpa/FPY, thus the shielding capabilities of the breeding/blanket and manifold structures are sufficient to guarantee the integrity of the VV over the 6 FPY DEMO lifetime.
- the main nuclear responses evaluated on EUROFER reach the following peak values at the FW: ~9.2 W/cm^3 nuclear heating density, ~10 dpa/FPY damage, 100 appm/FPY He-production.

The new 2016 WCLL breeding blanket design is based on a SMS approach, thus the single breeding unit (e.g. the volume enclosed between two neighboring stiffening plates) is recursively repeated along the poloidal direction, composing a single module for the inboard and outboard respectively.

The implementation of the SMS WCLL DEMO MCNP structure has been performed eliminating the gaps between the modules that were present in the model used so far, obtaining two empty single sectors. Successively the CAD model of the inboard and outboard SMSs have been preprocessed using the 3D modeling software ANSYS SpaceClaim 2017.1 [15] and converted into the equivalent MCNP geometries by means of the Multi-Physics Coupling Analysis Modeling Program MCAM [16]. The inboard and outboard MCNP models of the SMSs have been finally integrated with the DEMO MCNP model obtaining the SMS WCLL DEMO MCNP (Fig. 11).

The new SMS WCLL blanket module layout is characterized by cooling pipes with a helicoidal path in the FW area: the MCNP representation of such elements is quite complicated and it would require the definition of non-analytic surfaces that are not currently available in the code. Thus, the SMS layout was defined in the MCNP model through a proper radial segmentation (see TABLE I): each sector has been filled using a specific homogenized compound, with volume percentages of the materials (Eurofer, H_20, LiPb) extracted by the engineering CAD files. As far as the inboard SMS blanket is concerned, the same radial segmentation has been applied, considering the reduced radial extension of the breeding area. The calculations to assess the nuclear performances of the SMS design are presently ongoing: taking in consideration the reduced radiation streaming due to the gaps removal and the extended breeding area, an enhancement must be expected both in terms of tritium production and in shielding effectiveness on the TFC.

IV. Thermal-hydraulic Activities

A. First Wall and Breeding zone thermal-hydraulic analysis

A detailed thermal-hydraulic analysis of WCLL BB 2016 design [6], [7] was performed to investigate the coolant systems efficiency, ensuring that the temperature requirement of the structures is met. With the scope of obtaining an exhaustive temperature distribution both in fluid (i.e. PbLi, water) and solid domains (i.e. EUROFER structures and tungsten layer), a complete CFD model of the basic breeding unit [8] was developed. Several simulations were carried out, using ANYS CFX v.15 code, to evaluate the effect of boundary conditions and to optimize the thermal field.

The mesh consists of hexahedral and tetrahedral elements, and it is characterized by $14 \cdot 10^6$ nodes and $28 \cdot 10^6$ elements. Many local controls are used to properly resolve the geometrical features. The number of cells is inflated near the solid walls for to achieve the required resolution in the viscous sub-layer (y_1+=1). The SST k-ω turbulence model has been chosen for all the performed simulations. Despite the geometrical complexity of the model, a satisfactory result has been achieved in terms of mesh quality, with an average orthogonal quality of 0.83 and an average skewness of 0.29.

Each breeding unit includes 10 cooling channels in the FW, where water flows in counter-current direction along a radial-toroidal-radial path. The BZ coolant system is constituted by 21 cooling Double Wall Tubes (DWTs), with water flowing in the radial-toroidal direction. BZ water enters the 10 tubes nearby the FW, it is mixed in the manifold and then it recirculates in the other 11 tubes in the opposite direction, as depicted in Fig. 12. This BZ water flow path allows to increase the coolant velocity and to obtain an almost symmetrical temperature distribution in the toroidal direction. The PbLi flows in the six channels, defined by the radial-poloidal stiffeners, along the radial-poloidal direction.

The CFD calculations have been performed considering a nominal Heat Flux (HF) of 0.5 MW/m^2 at the interface of tungsten/plasma, to simulate the power deposition on the FW surface due to particles and radiations. Moreover, a volumetric

power density, radially distributed, is applied to the solid domains (FW and stiffeners) and to the PbLi domain, to simulate the nuclear heating. The total power in the elementary breeder cell volume is 3.46 MW, distributed as follows: 1.27 MW in the FW, and 2.19 MW in the BZ. Considering that water of both coolant systems enters at 15.5 MPa and 285°C, the total inlet mass flow rate is 1.529 kg/s. The PbLi inlet mass flow rate is 0.140 kg/s and the inlet temperature is 325 °C. Buoyancy forces are considered in the PbLi domain. A 0 Pa relative pressure is set on the outlet surfaces of fluid domains (i.e. FW and BZ coolant, and PbLi).

The PbLi and water material properties (i.e. density, viscosity, and heat capacity at constant pressure) are implemented in the CFX input as temperature-dependent [7].

The results of CFD analyses show that the maximum temperature in the solid domains is well below the limit (550 °C), as illustrated in Fig. 13. The BZ and FW coolant systems performances are satisfactory, with a maximum bulk temperature of 336°C in the FW and 324 °C in the BZ system. The maximum BZ coolant velocity recorded is 2.78 m/s, far below the limit of 7 m/s assumed to limit the corrosion of the EUROFER pipes, leaving a consistent margin to further enhance the cooling system efficiency [4]. Moreover, the analyses showed the presence of a relevant asymmetry of the PbLi temperature distribution in the toroidal direction (see Fig. 14). This issue is related to the BZ coolant system layout, which shall be simplified.

Starting from the main feedbacks of the CFD analyses of WCLL BB 2016 design, further investigations have been performed, with the aim of enhancing the symmetry of the thermal field, improving coolant systems performances, and simplifying the BZ coolant system layout. Fig. 15 shows one of the configurations studied in 2017. In this BZ coolant system layout, the number of tubes is reduced from 21 to 6, enhancing the cooling performances. Moreover, the coolant system is simplified, as the tubes are inserted in the toroidal channels without crossing the radial-poloidal stiffeners.

Preliminary analyses demonstrate that the symmetry of temperature field in toroidal direction is improved, and the maximum temperature is still below the limit, as shown in Fig. 16, where the PbLi thermal field is shown.

Further analyses are ongoing to study in depth the configuration selected, also in terms of thermo-mechanical response, and to investigate other BZ coolant system layouts.

B. Breeding zone MHD analysis

To ensure the fulfillment of the design requirements, the liquid metal hydraulic path in the BB component must be studied considering the effects introduced by the magnetic field which include, but are not limited to, dramatic flow pattern variation, turbulence suppression and severe MHD-related pressure drops [17].

In the WCLL BB Design 2016, DWTs carry the coolant required to refrigerate the BZ. The pipes are transverse to the main flow direction in the elementary cell except for the two lateral channels, where they are aligned. Building upon the experience obtained in the characterization of the MHD flow for the simplified elementary channel [18], a study was conducted to assess the influence of these obstacles on pressure drops and heat transfer performance [19], [20].

The test section modeled in the CFD code ANSYS CFX is shown in Fig. 17 and it is representative of the area surrounding a single pipe in the WCLL Design 2016. The duct walls are conductive with non-uniform thickness, which leads to the creation of regions in the duct cross-sections with huge differences in the arising electromagnetic drag [18]. The flow is assumed to be laminar. The duct mean velocity calculated at the inlet for the simulations performed is in the range $Re = [20, 80]$.

To evaluate the effect of the pipe presence on the channel pressure drops, a pressure penalty index (p_o) was employed, which is defined as

$$p_o(\%) = \frac{\Delta p - \Delta p_{2D}}{\Delta p_{2D}} \quad (1)$$

where Δp_{2D} is the pressure drop of the unperturbed flow, obtained from the calculated pressure gradient in fully developed flow and the test section axial length. The pressure penalty was found to decrease monotonically with the intensity of the magnetic field (B_0), reaching 10% for a Hartmann number (M) equal to 430 [20]. The reason for this behavior is the stronger dependence on B_0 of the fully developed pressure drop term ($\Delta p_{2D} \propto B_0^2$, electro-conductive duct walls) compared with the obstacle term, which is roughly a linear function of the magnetic field intensity [17]. Likewise, the effect of the obstacle conductivity is limited for $M \to \infty$ [19]. Therefore, it is safe to assume that for the magnetic field design intensity ($M \simeq 10^4$) the pipes presence would have no effect on the elementary cell pressure drop.

Regarding the heat transfer, the Nusselt number was found to increase with the magnetic field intensity in the analyzed range as shown in Fig. 18. This increase is explained with the promotion of the mass flow in the sub-channel below the cylinder, due to the electromagnetic drag not being dependent on the flow cross-section, as opposed to the hydraulic one. For the $Re = 20$ case, just the 6% of the total flow rate is carried by the bottom sub-channel in a hydrodynamic flow whereas this value steadily increases with M, reaching 25% at $M = 430$. The improvement is sufficient to compensate the heat transfer reduction due to the suppression of the wake vortex structures that, for all the cases considered, are dissipated by the magnetic field action with the reversion to a creeping flow regime, otherwise observed just for $Re \to 0$ [20].

The obstacle electrical conductivity has a negligible influence on the heat transfer for the considered range. The maximum difference of the Nusselt number between the two limiting cases of perfectly insulated and perfectly conducting cylinder surface is 3% for the considered range considered of the Hartmann number M [19].

In conclusion, the obstacle presence does not affect considerably the MHD pressure drops in the elementary cell of

the WCLL BB Design 2016. Conversely, a slight increase ($\simeq 20\%$) in the heat transfer compared with the pure hydrodynamic case has been observed. Further investigation is required to confirm this enhancement for magnetic field intensity closer to the operative value $M = O(10^4)$.

Follow-up activities are ongoing focusing on the investigation of the buoyancy forces role in this configuration. Although initially neglected in the described results, previous CFD studies have shown their influence on the PbLi temperature distribution in the hydrodynamic case.

V. Thermo-Mechanical Activities

Within the framework of EUROfusion activities regarding the DEMO Breeding Blanket (BB) design, University of Palermo is in charge to perform the thermo-mechanical assessment of the DEMO WCLL BB [6], [7], [21]–[26]. The purpose of this activity is to develop a feasible and reliable design, able to safely withstand the thermal and mechanical loads the module undergoes during normal and accidental operative scenarios while giving fruitful feedbacks to the other groups (neutronic, thermal-hydraulic, CAD, etc.) involved in the DEMO WCLL BB R&D activities. A considerable part of the R&D activity performed at the University of Palermo in 2016 has concerned the analysis of the thermo-mechanical performances of a typical 20° sector of the DEMO WCLL BB. The study has been performed following a numerical approach based on the Finite Element Method (FEM) and adopting the commercial ABAQUS v. 6.14-2 FEM code

Attention has been paid to the assessment of the sector thermo-mechanical behavior under Normal Operation (NO) and Central Major Disruption (CMD) steady-state loading scenarios, in order to check the fulfillment of the prescribed SDC-IC criteria [27], [28]. In particular, NO scenario foresees the nominal loading conditions envisaged for the DEMO WCLL BB, whereas in the CMD scenario, Electro-Magnetic (EM) loads, originated by a plasma central major disruption event, are considered in addition to nominal ones.

The geometric design of a typical DEMO WCLL breeding blanket 20° sector (Fig. 19) consists in three Outboard Blanket (OB) segments, namely the Right (OBR), the Central (OBC) and the Left (OBL) segment, plus two Inboard Blanket (IB) segments, namely the Right (IBR) and the Left (IBL) one. For the purpose of this study, segments conceived according to the Multi-Module concept have been considered. Therefore, each segment is composed of 7 modules directly tied to the BSS. Furthermore, the attachment system (Fig. 20) devoted to connecting the BSS to the Vacuum Vessel (VV) has been considered, properly taking into account the keys (in yellow in Fig. 19 and Fig. 20) with the respective housings (in blue in Fig. 19 and Fig. 20), the upper port plug, the equatorial pads and the poloidal spring.

As to the FEM model, a mesh composed by ~900k nodes connected in ~1.5M hexahedral and tetrahedral linear elements has been set-up realistically reproducing the BB sector, the BSS and the attachment system as a whole. To save computational resources and speed-up calculation time, blanket modules have been modified as "dummy" modules, consisting of solid blocks without any internal structure. The EUROFER steel has been assumed as the structural material. Regarding blanket modules, as they are “dummy” components, effective EUROFER thermo-mechanical properties have been implemented to take into account the change in stiffness due to their modeling strategy. In particular, Young’s modulus values equal to one-tenth of the actual ones have been assumed in order to reproduce the actual modules stiffness. Moreover, equivalent density values have been purposely calculated and adopted in order to consider the actual breeder and steel masses within IB (9032.5 kg/m^3) and OB (10393.6 kg/m^3) modules.

Regarding NO scenario, gravity and thermal loads have been imposed. Concerning the thermal field (Fig. 21), a linearly decreasing radial temperature profile, varying from 500 °C on the plasma facing surface down to 300 °C at the modules back-plate, has been considered. Furthermore, BSS, keys and upper port plug have been considered at 300 °C, whereas key housings (not shown in Fig. 21) have been assumed at 200 °C, according to the temperature currently envisaged for the VV.

Interactions between keys and housings, BSS and upper port plug as well as between OB segments and equatorial pads have been simulated adopting a proper contact model, characterized by a Coulombian friction coefficient assumed to be equal to 0.25.

About the mechanical restraints, radial and toroidal displacements have been prevented to all the housing nodes. Concerning poloidal displacements, proper values have been calculated and imposed to the housings to simulate the VV thermal expansion except for bottom key housings, whose poloidal displacement has been set to 0 as they are at ground level. Lastly, a preliminary analysis has allowed to set-up the non-linear spring characteristic curve.

Concerning CMD scenario, the EM loads (Maxwell’s and Lorentz’s concentrated forces and moments) provided by KIT have been applied together with the loads, interactions and boundary conditions already considered in the NO scenario. EM loads have been applied to the centers of mass of modules and BSS regions.

A campaign of preliminary parametric analyses, not described for the sake of brevity, has been performed in order to assess the initial keys-housings gaps, along radial, toroidal and poloidal directions, to be considered as mandatory to ensure the accommodation of thermal expansion during the NO scenario. Once determined these gaps, steady-state thermo-mechanical analyses under NO and CMD scenarios have been run.

Results in terms of displacement are shown in Fig. 22. It is possible to observe that OB displacement values are generally higher than IB ones. This means that, in both scenarios, OB deforms more than IB. Furthermore, as to CMD scenario, quite huge displacements within IB upper modules, in the proximity of IB bend region, are calculated. Therefore, a partial overlapping among these modules is predicted. This behavior may depend on the EM loads amount together with the combined effect of the IB shape and the attachment system action. In fact, in this IB region, BSS thickness achieves its

minimum value offering the lowest mechanical resistance to the module deformation.

The Von Mises equivalent stress field arising within the BSS under both scenarios investigated is depicted in Fig. 23. The most stressed regions are located, in both scenarios, in correspondence of the BSS knees. Concerning NO scenario, highest stress is predicted within the thinnest IB BSS region. As to CMD scenario, other quite stressed regions are located approximately in the middle of the different BSS regions, nearby their centers of mass. High stresses arising within these regions are mainly originated by the modeling choice to apply EM loads as concentrated forces and moments to the centers of mass.

Finally, in order to verify the fulfillment of the SDC-IC most critical criterion, namely that against immediate plastic flow localization $(P+Q)_m/S_e$ [28], the paths are shown in Fig. 24, located within the BSS most stressed knees, have been considered. Results of the SDC-IC most critical criterion verification are reported in TABLE II. It is remarkable that the criterion is totally fulfilled under both loading scenarios assessed.

In conclusion, results obtained seem to indicate that a revision of the DEMO WCLL BB sector geometric design, in particular, the upper inboard and outboard regions, is necessary in order to avoid the arising of non-homogeneous displacement which entails modules overlapping. In addition, also the attachment system should be carefully revised since it plays a non-negligible role in the sector deformation process.

Moreover, a more detailed EM loads assessment and modeling are strongly suggested to perform a more accurate thermo-mechanical analysis under CMD loading scenario.

VI. PHTS Integration and Balance Of Plant (BOP)

A. PHTS Integration

The main function of the PHTS is to provide cooling water to the first wall and blanket modules and to transfer the thermal power to the Power Conversion System (PCS). The WCLL BB sector is linked with the PHTS through the in-vessel piping system, which is formed by the feeding and collecting pipes of the two inboard and three outboard segments [6]. All the pipes of one sector enter and exit through the upper port, as shown in Fig. 25. The preliminary sizing of EUROFER pipelines dimensions is performed according to the velocity limit of 7 m/s.

Considering the reference thermodynamic cycle (i.e. water inlet temperature 295 °C, and outlet temperature 328 °C), the overall primary system mass flow rate which is feeding the whole reactor is 10561 kg/s.

The WCLL PHTS is constituted by two independent systems: the BZ primary system and the FW primary system. During the pulse mode, the BZ primary system delivers the power (1577 MW_{th}) to the turbine by means of Once-Through Steam Generators (OTSG). The FW primary system transfers the heat to the Energy Storage System (ESS) through two Intermediate Heat Exchangers (IHXs), using HITEC molten salt as fluid. The total power transferred from the FW to PHTS is 467.6 MW_{th}. During the dwell time, the ESS transfers the heat, accumulated during the pulse mode, to four Steam Generators. The two independent primary systems are represented in Fig. 26, showing the two OTSGs, the pressurizer (PRZ) of BZ and FW systems, the two IHXs water-HITEC, and the main coolant pumps.

The cooling water is distributed and collected by means of four ring headers, hosted in a proper passage 7×7 m that runs all around the tokamak. The main pipeline diameters outside the vacuum vessel are calculated accounting for coolant velocity of 15 m/s, with a maximum limit of 20 m/s.

The primary coolant is pressurized by means of a pressurizer connected to the hot leg upstream of the steam generator. The type and location of this pressurizer were selected based on space considerations, pressure controllability, and safety criteria.

Starting from the preliminary sizing, the FW and BZ primary system CAD models have been developed and integrated with DEMO baseline CAD. The location of the main PHTS components with respect the tokamak building can be seen in Fig. 27.

B. BOP

The thermodynamic cycle hypothesized is derived from the PWR cycles with OTSGs and it is shown in Fig. 28. The steam turbine is moved by superheated steam (299 °C at 6.4 MPa) made into the OTSGs during the pulse mode and into the Molten Salt Steam Generator (MS-SG) during the dwell mode.

The MS-SG is part of ESS and it produces steam mainly during the dwell using the energy from the FW, stored during the pulse phase as sensible heat by the molten salt.

Thanks to this double steam source, the steam turbine works with a small variation of main parameters between the two operational modes. Consequently, the turbine life is expected longer than the DEMO life. This is a conservative assumption and, in future, R&D is planned for a reduction of the ESS dimension (or elimination).

Three feed-water preheaters are substituted by a heat recovery from divertor and vacuum vessel, though the correspondent PHTS for an efficiency increment.

A Gatecycle™ analysis, based on previous studies by Malinowski et al. [29] and updated with the new configuration was carried out, mainly focused on the efficiency estimation. The preliminary result is about 36% mean gross electrical efficiency, considering both pulse and dwell phases.

The electrical efficiency is reduced to 34%, with the consideration of the electrical load (limited to PHTSs, ESS and BoP components for this analysis).

VII. Conclusions

The paper describes the status of the WCLL BB conceptual design. The CAD model of WCLL BB inboard and outboard segments is available, including the BSS, manifolds, and the integration with the PHTS. Detailed analyses were performed to support design choices, and to demonstrate the reliability of the design. In the paper, the main results outlined were:

- Integrated FW performance is able to sustain the average heat flux ($\simeq 0.5\ MW/m^2$) considered in the DEMO-2015. Further studies will be performed in 2017 based on more detailed loads specifications.
- Themo-hydraulic analyses, carried out focusing on the elementary breeding unit, demonstrated that the FW and BZ systems have satisfactory coolant efficiencies with margin for improvements. Analyses, aimed at optimizing and simplifying the BZ system layout, are in progress.
- Heterogeneous neutronic analyses performed on the WCLL BB Design 2015 (based on the MMS approach) confirmed the meeting of all the requirements. Homogeneous neutronic analyses based on the SMS concept are actually ongoing-
- CFD analyses were performed to assess the influence of the BZ cooling pipes on MHD pressure drops. The 3D pressure drop term due to channel cross-section variation was found to quickly become negligible with increasing Hartmann number. Increases in the heat transfer due to flow pattern variation, promoted by the magnetic field, was observed.
- Thermo-mechanical analyses for both the IB and OB modules were performed in two relevant operational scenarios: NO and CMD. Design requirements are fulfilled for the conditions considered.

REFERENCES

[1] F. Romanelli *et al.*, "Fusion Electricity - A roadmap to the realisation of fusion energy," *EFDA*, 2012.

[2] L. V. Boccaccini *et al.*, "Objectives and status of EUROfusion DEMO blanket studies," *Fusion Eng. Des.*, vol. 109–111, pp. 1199–1206, 2015.

[3] G. Federici *et al.*, "Overview of the design approach and prioritization of R&D activities towards an EU DEMO," *Fusion Eng. Des.*, vol. 109–111, pp. 1464–1474, 2016.

[4] P. Sardain *et al.*, "Power plant conceptual study - WCLL concept," *Fusion Eng. Des.*, vol. 69, no. 1–4 SPEC, pp. 769–774, 2003.

[5] J. Aubert, G. Aiello, N. Jonquères, A. Li Puma, A. Morin, and G. Rampal, "Development of the Water Cooled Lithium Lead blanket for DEMO," *Fusion Eng. Des.*, vol. 89, no. 7–8, pp. 1386–1391, 2014.

[6] A. Del Nevo *et al.*, "WCLL breeding blanket design and integration for DEMO 2015: status and perspectives," *Fusion Eng. Des.*, vol. 124, pp. 682–686, 2017.

[7] E. Martelli *et al.*, "Advancements in DEMO WCLL breeding blanket design and integration," *Int. J. Energy Res.*, 2017.

[8] R. Mozzillo, A. Del Nevo, E. Martelli, and G. Di Gironimo, "Rationale and method for design of DEMO WCLL breeding blanket poloidal segmentation," *Fusion Eng. Des.*, vol. 124, pp. 664–668, 2017.

[9] R. Mozzillo, D. Marzullo, A. Tarallo, C. Bachmann, and G. Di, "Development of a master model concept for DEMO vacuum vessel," *Fusion Eng. Des.*, vol. 112, pp. 497–504, 2016.

[10] R. Mozzillo, A. Tarallo, D. Marzullo, C. Bachmann, G. Di, and G. Mazzone, "Preliminary structural assessment of DEMO vacuum vessel against a vertical displacement event," *Fusion Eng. Des.*, vol. 112, pp. 244–250, 2016.

[11] U. Fischer *et al.*, "Neutronic analyses and tools development efforts in the European DEMO programme," *Fusion Eng. Des.*, vol. 89, no. 9–10, pp. 1880–1884, 2014.

[12] U. Fischer *et al.*, "Neutronic performance issues of the breeding blanket options for the European DEMO fusion power plant," *Fusion Eng. Des.*, vol. 109–111, pp. 1458–1463, 2015.

[13] X-5 Monte Carlo Team, *MCNP - A General Monte Carlo N-Particle Transport Code, Version 5, Los Alamos, New Mexico, USA*. 2003.

[14] "JEFF-3.2 evaluated data library – neutron data, OECD-NEA." [Online]. Available: https://www.oecdnea.org/dbforms/data/eva/evatapes/jeff 32/.

[15] "Ansys SpaceClaim Engineering 2017." [Online]. Available: www.spaceclaim.com.

[16] Y. Wu, "CAD-based interface programs for fusion neutron transport simulation," *Fusion Eng. Des.*, vol. 84, no. 7–11, pp. 1987–1992, 2009.

[17] S. Smolentsev, R. Moreau, L. Bühler, and C. Mistrangelo, "MHD thermofluid issues of liquid-metal blankets: Phenomena and advances," *Fusion Eng. Des.*, vol. 85, no. 7–9, pp. 1196–1205, 2010.

[18] A. Tassone, G. Caruso, A. Del Nevo, and I. Di Piazza, "CFD simulation of the magnetohydrodynamic flow inside the WCLL breeding blanket module," *Fusion Eng. Des.*, vol. 124, pp. 705–709, 2017.

[19] A. Tassone, M. Nobili, and G. Caruso, "Magnetohydrodynamic flow and heat transfer around a heated cylinder of arbitrary conductivity," *J. Phys. Conf. Ser.*, vol. 923, no. 1, p. 12024, 2017.

[20] A. Tassone, M. Nobili, and G. Caruso, "Numerical study of the MHD flow around a bounded heating cylinder: heat transfer and pressure drops," *Int. Commun. Heat Mass Transf.*, 2018. (in pubblication)

[21] P. A. Di Maio, P. Arena, G. Bongiovì, P. Chiovaro, A. Del Nevo, and R. Forte, "Optimization of the breeder zone cooling tubes of the DEMO Water-Cooled Lithium Lead breeding blanket," *Fusion Eng. Des.*, vol. 109–111, pp. 227–231, 2016.

[22] P. A. Di Maio, P. Arena, G. Bongiovì, P. Chiovaro, A. Del Nevo, and M. L. Richiusa, "On the thermo-mechanical behaviour of DEMO water-cooled lithium lead equatorial outboard blanket module," *Fusion Eng. Des.*, vol. 124, pp. 725–729, 2017.

[23] P. A. Di Maio *et al.*, "Structural analysis of the back supporting structure of the DEMO WCLL outboard blanket," *Fusion Eng. Des.*, pp. 10–13, 2016.

[24] P. Chiovaro *et al.*, "Assessment of the Thermo-mechanical Performances of a DEMO Water-Cooled Liquid Metal Blanket Module," *J. Fusion Energy*, vol. 34, no. 2, pp. 277–292, 2015.

[25] P. A. Di Maio *et al.*, "Analysis of the thermo-mechanical behaviour of the DEMO Water-Cooled Lithium Lead breeding blanket module under normal operation steady state conditions," *Fusion Eng. Des.*, vol. 98–99, pp. 1737–1740, 2015.

[26] P. A. Di Maio, P. Arena, G. Bongiovì, P. Chiovaro, R. Forte, and S. Garitta, "On the optimization of the first wall of the DEMO water-cooled lithium lead outboard breeding blanket equatorial module," *Fusion Eng. Des.*, vol. 109–111, no. PartA, pp. 335–341, 2016.

[27] F. Tavassoli, "Fusion Demo Interim Structural Design Criteria (DISDC), Appendix A Material Design Limit Data: A3. S18E Eurofer Steel, EFDA TASK TW4-TTMS-005-D01. CEA Report DMN/DIR/NT/2004-02/A," 2007.

[28] "ITER Structural Design Criteria for In-vessel components (SDC-IC)." .

[29] L. Malinowski, M. Lewandowska, and F. Giannetti, "Analysis of the secondary circuit of the DEMO fusion power plant," *Fusion Eng. Des.*, pp. 3–6, 2017.

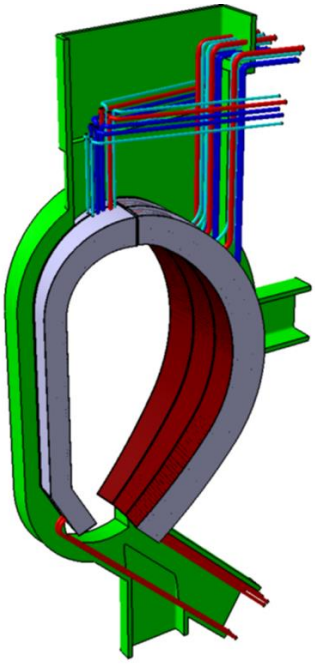

Fig. 1 DEMO sector piping system

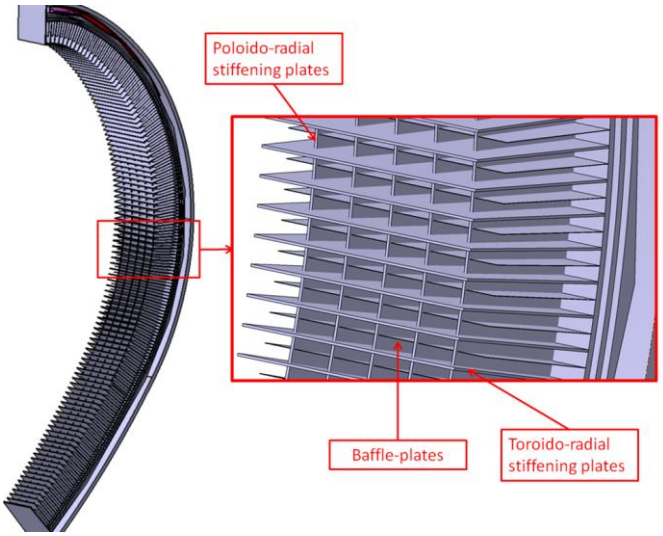

Fig. 2 WCLL BB module internal structure

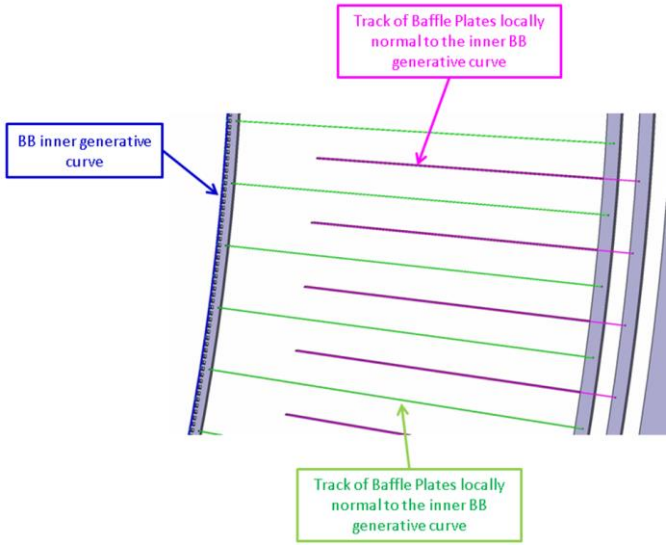

Fig. 3 Track of baffle plates and TR stiffening plates

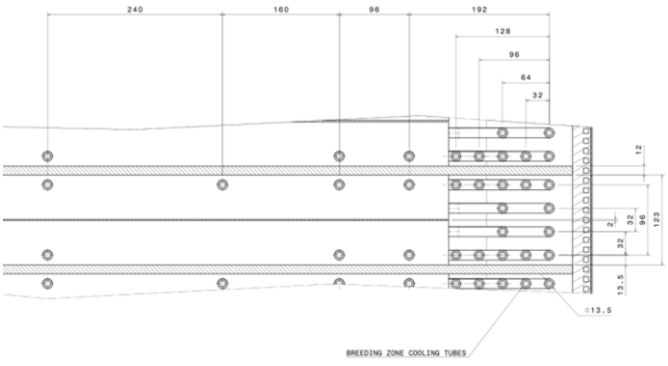

Fig. 4 Layout of BZ cooling tubes on an elementary cell

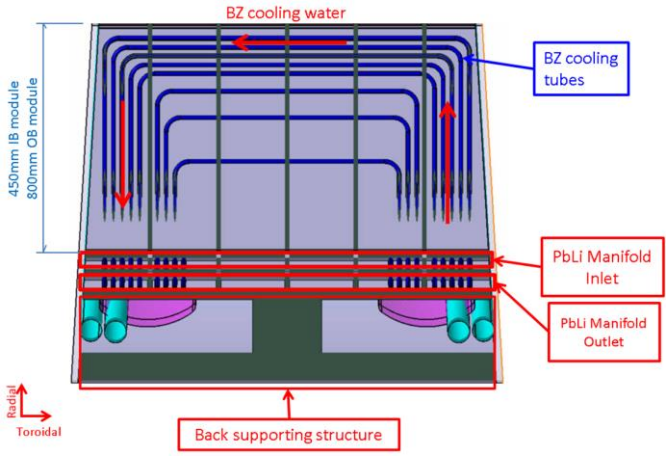

Fig. 5 Section of the single module on toroidal-radial plane

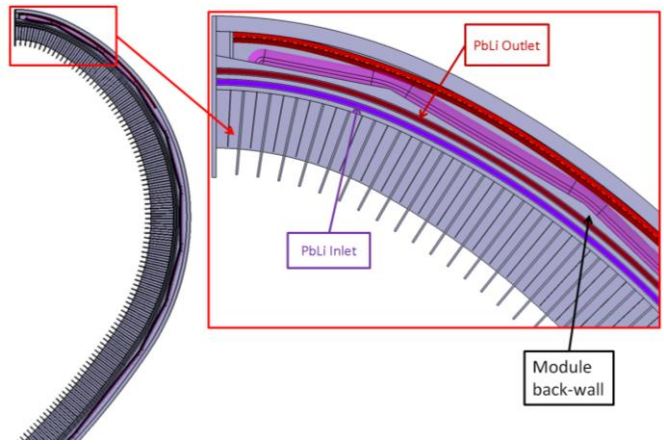

Fig. 6 Back-wall and Pb Li manifold region

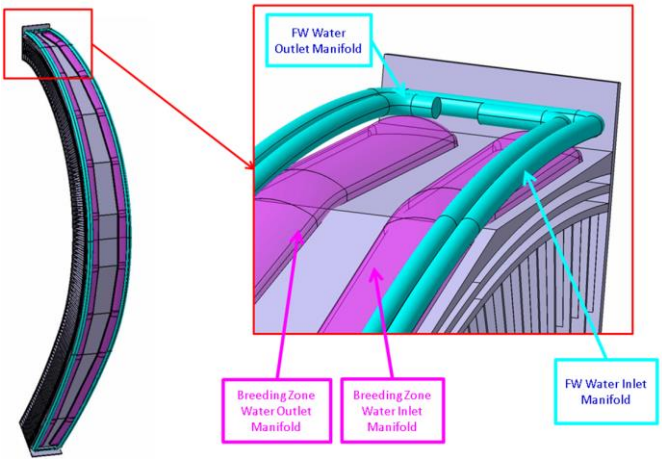

Fig. 7 BZ and FW cooling water manifold

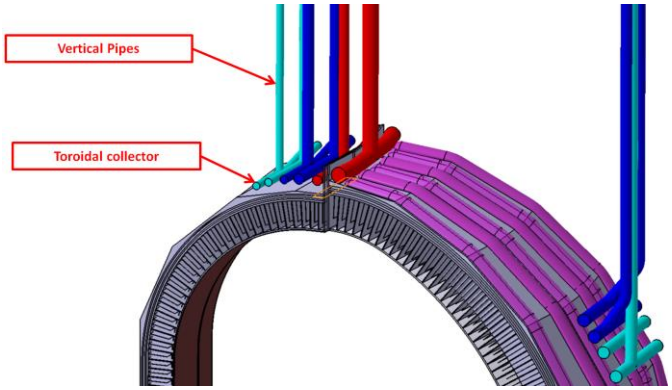

Fig. 8 BB sectors feeding system with toroidal collectors in the upper port area

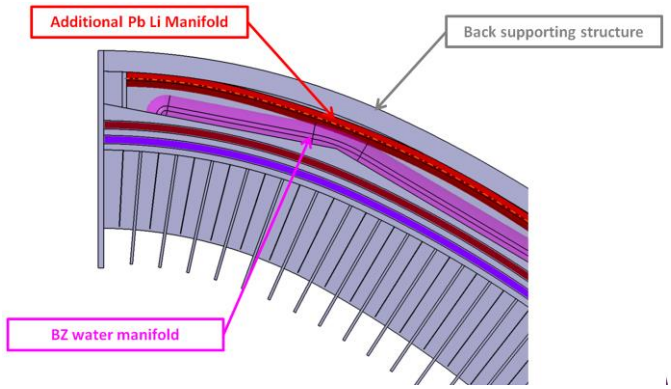

Fig. 9 Additional manifold layout

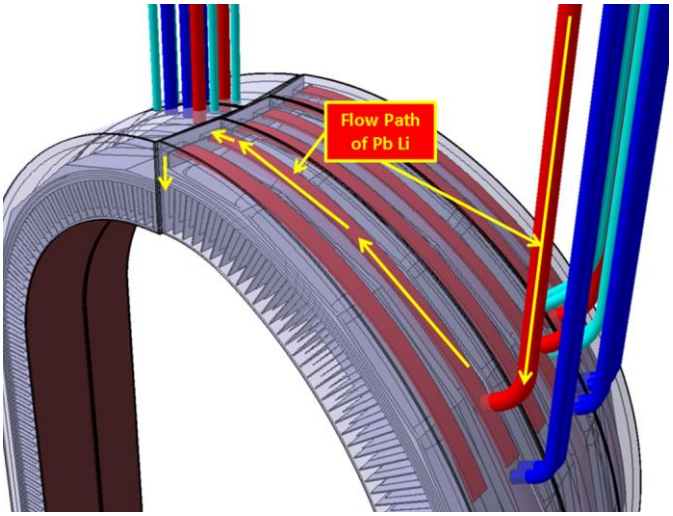

Fig. 10 Flow path of Pb Li in the outboard segments

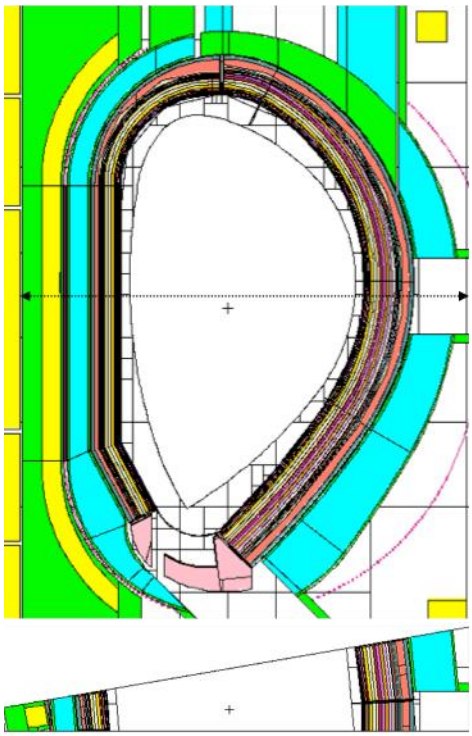

Fig. 11 SMS WCLL DEMO MCNP model: poloidal section showing the inboard and outboard breeding blanket single segment (upper panel) and toroidal section across the equatorial plane (lower panel).

TABLE I
RADIAL SEGMENTATION OF THE OUTBOARD SMS WCLL BB MCNP MODEL

Component	Thickness (mm)	Material composition (%) W	LiPb	H_20	Eurofer
W layer	2	100	0	0	0
First Wall	3	2.03	0	0	97.97
	7	1.07	0	50.20	48.73
	15	0.66	0	1.64	97.70
Breeding Zone	25	0.45	84.26	0.89	14.40
	14	0.37	58.61	10.41	30.61
	32	0.32	80.53	2.87	16.27
	32	0.29	75.88	4.62	19.21
	32	0.12	81.09	2.87	15.92
	32	0	81.10	2.91	15.99
	80	0	78.13	1.83	20.04
	80	0	77.87	1.86	20.28
	80	0	79.08	1.41	19.51
	80	0	78.50	1.65	19.86
	80	0	79.08	1.44	19.48
	80	0	79.16	1.43	19.41
	80	0	78.00	1.88	20.12
	73	0	78.98	1.52	19.50
LiPb Manifolds	30	0	0	0	100
	40	0	38.23	0	61.77
	30	0	0.00	0	100
	40	0	38.18	0	61.82
Back Plate	30	0	0	0	100
Manifolds	200	0	0	93.36	6.64
Back Supporting Structure	100	0	0	0	100

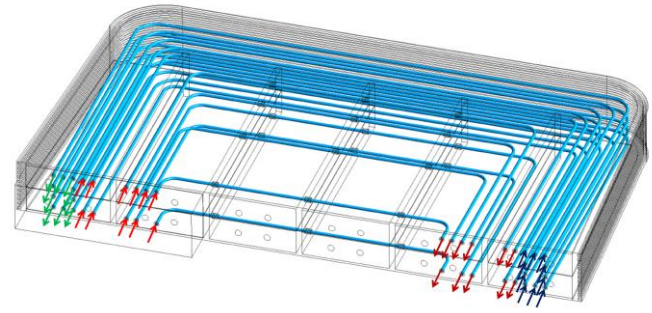

Fig. 12 WCLL breeding unit: BZ coolant system layout

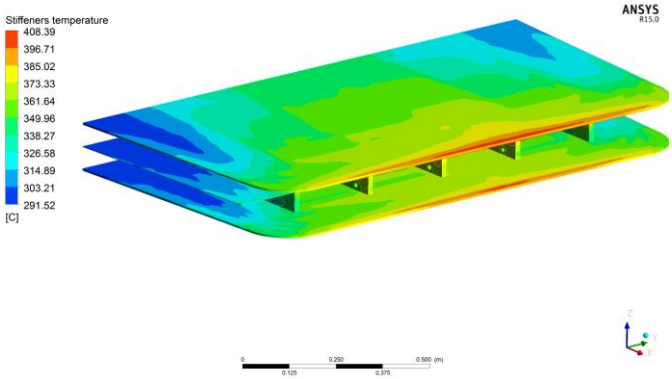

Fig. 13 CFD analyses of WCLL BB 2016 design: stiffeners temperature.

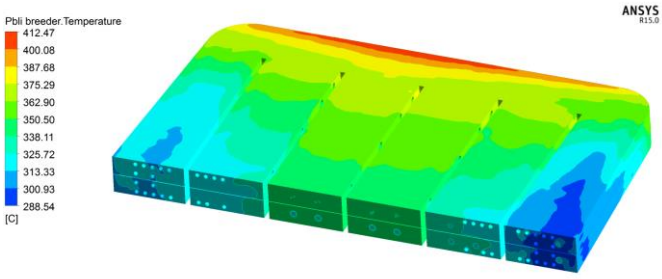

Fig. 14 CFD analyses of WCLL BB 2016 design: PbLi temperature.

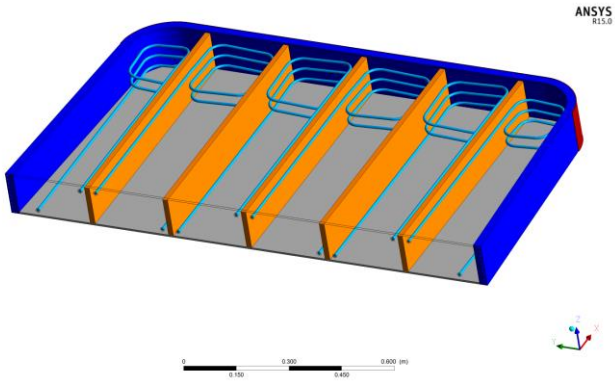

Fig. 15 WCLL BB 2017 design: BZ coolant system layout.

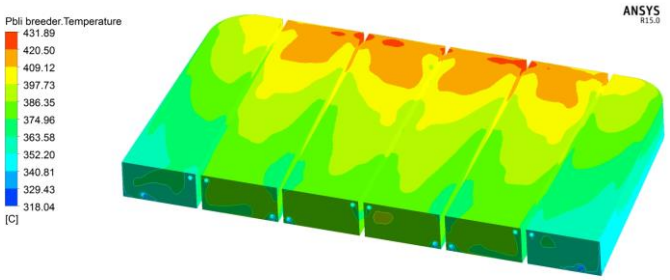

Fig. 16 CFD analysis of WCLL BB 2017 design: PbLi temperature

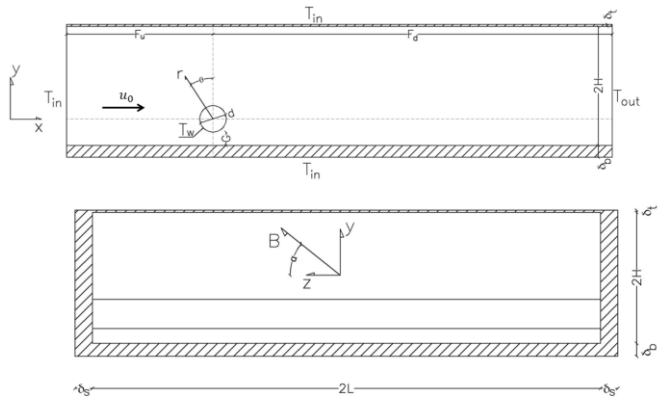

Fig. 17 BZ MHD analysis test section. Top: radial-poloidal cross-section, bottom: toroidal-poloidal cross-section.

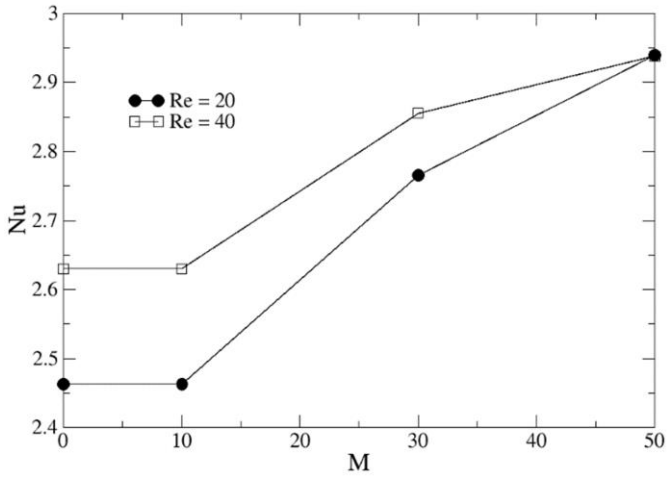

Fig. 18 Nusselt number as a function of the magnetic field intensity expressed with the Hartmann number. The plot refers to perfectly insulating obstacle ($c_o = 0$).

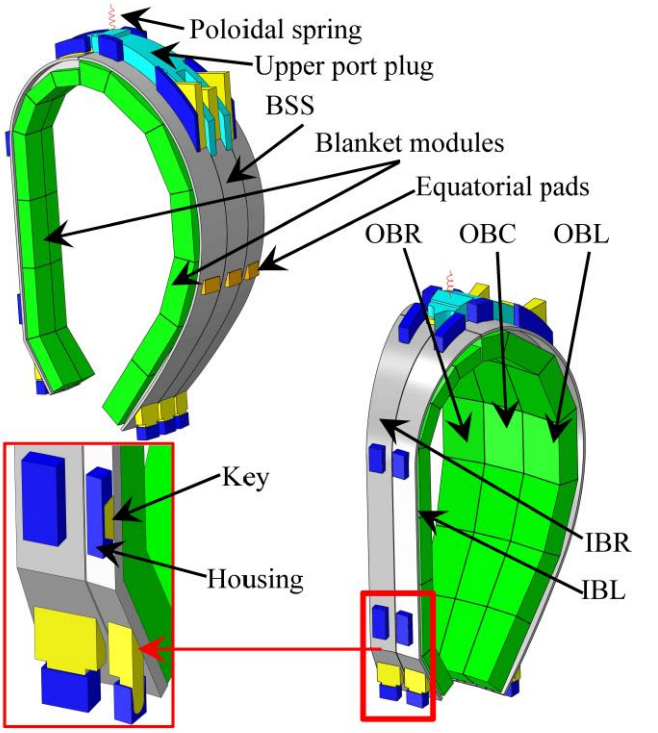

Fig. 19 DEMO WCCL breeding blanket 20 ° sector geometric configuration.

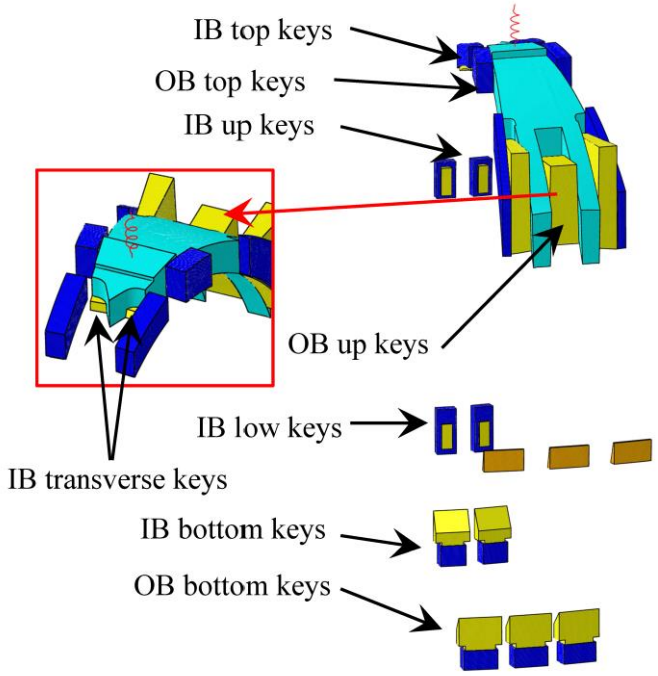

Fig. 20 The attachment system.

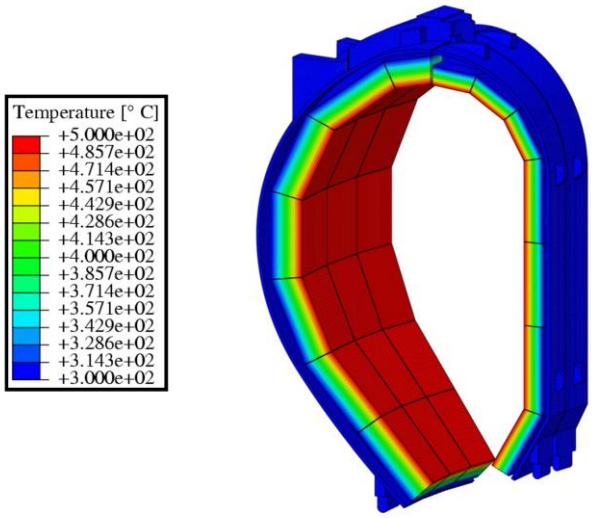

Fig. 21 The imposed thermal field.

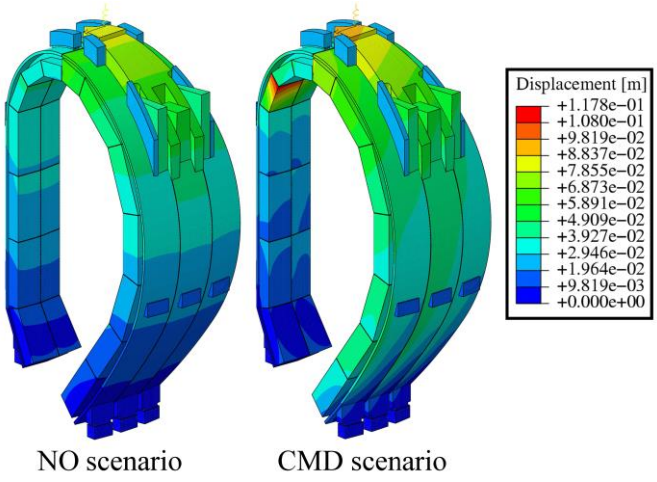

Fig. 22 Displacement field under NO and CMD scenarios.

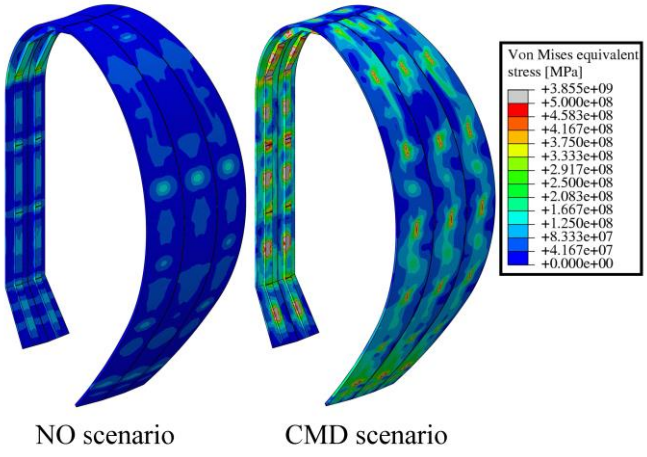

Fig. 23 Von Mises equivalent stress field under NO and CMD scenarios.

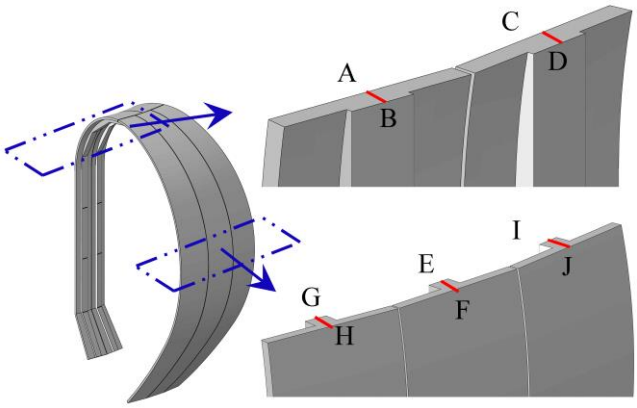

Fig. 24 Paths for the SDC-IC criterion verification.

TABLE II
$(P+Q)_m/S_e$

Path	NO scenario	CMD scenario
AB	0.27	0.85
CD	0.26	0.81
EF	0.15	0.18
GH	0.14	0.17
IJ	0.14	0.25

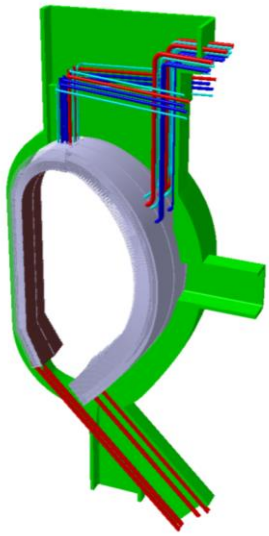

Fig. 25 WCLL Breeding Blanket and PHTS integration.

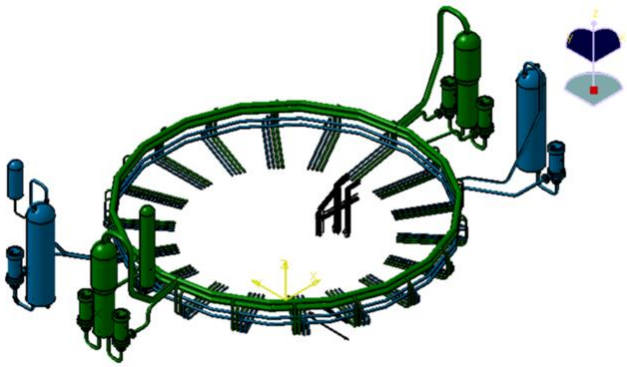

Fig. 26 Breeding Zone and First Wall Primary Heat Transfer System

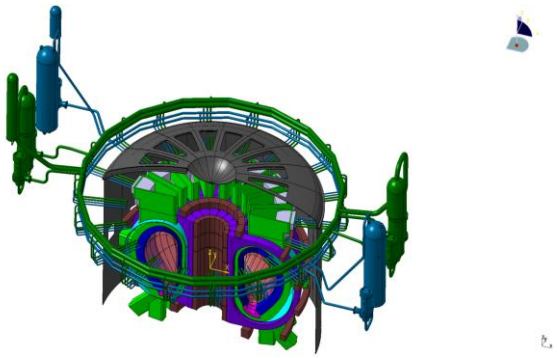

Fig. 27 Integration of WCLL PHTS with DEMO tokamak building

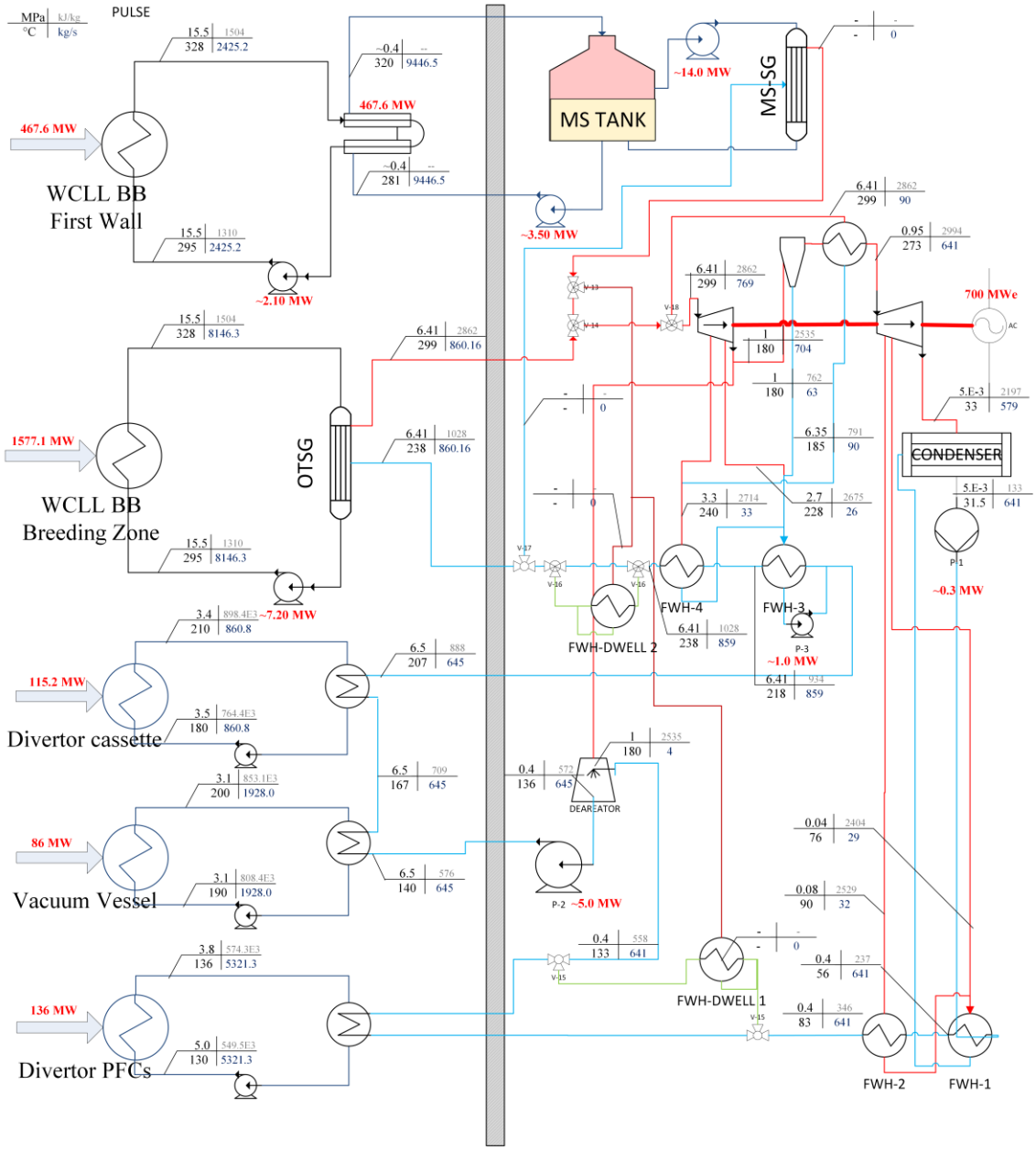

Fig. 28 Preliminary cycle configuration during pulse mode